

Heavy flavor machine learning algorithms for fast data processing in sPHENIX

Cameron Dean*, on behalf of the sPHENIX and FastML collaborations

¹Massachusetts Institute of Technology

Abstract. The sPHENIX experiment at RHIC utilizes the first new heavy ion detector since the switch on of the LHC experiments. It's optimized for precision jet and heavy flavor physics measurements, and recorded its first collisions in spring 2023. sPHENIX uses a tracking system with streaming readout and barrel calorimetry to reconstruct the collision topology. Event plane detectors, minimum bias detectors and zero-degree calorimeters are used to characterize the event. The streaming readout detectors are capable of recording 10% of the minimum bias rate, in addition to triggered events, in $p+p$ collisions which will enable unabated, precision b -hadron and heavy flavor jet measurements at RHIC. An AI-assisted hardware trigger demonstrator is under development to sample the remaining 90% of minimum-bias $p+p$ collisions with an aim for further deployment at the EIC.

1 Introduction

On May 18th 2023, the sPHENIX collaboration began operations and started recording Au+Au collisions at the first new heavy ion detector since the start of the LHC experimental program. sPHENIX consists of four tracking detectors, barrel electromagnetic and hadronic calorimeters, along with event plane detectors, minimum-bias detectors and zero-degree calorimeters to fully characterize Au+Au collisions. To enable precise momentum determination, sPHENIX uses a 1.4 T magnetic field in the barrel region. Combined with a state-of-the-art streaming readout (SRO) system from the tracking detectors, sPHENIX will complete the RHIC science mission with high statistics measurements from open charm, b -hadron and heavy flavor jets along side a wide array of other physics studies [1]. The SRO is designed to record 10% of the minimum bias rate in $p+p$ collisions, in additions to a 15 kHz jet trigger. A demonstrator module which employs machine-learning algorithms on field-programmable gate arrays (FPGAs) is under development to sample the remaining 90% of the collisions which will complement the base program of sPHENIX [2].

The innermost detector in sPHENIX is the monolithic active pixel sensor (MAPS) vertex detector (MVTX). The MVTX is a three-layer detector which allows precise vertex determination and primary/secondary vertex separation. It is capable of a track resolution of approximately $5\ \mu\text{m}$ and a 2D distance of closest approach (DCA) resolution of approximately $30\ \mu\text{m}$ for tracks with a p_T greater than 1 GeV and approaching $10\ \mu\text{m}$ with increasing p_T [3]. Further out radially is the intermediate tracker (INTT), a silicon-strip detector with a timing resolution of 106 ns. This matches the expected $p+p$ collision rate and hence allows for

*e-mail: ctdean@mit.edu

pile-up separation. Charged particles then pass through a compact time-projection chamber (TPC) which records clusters between 30 cm and 80 cm and uses an Argon/CF₄ gas mixture to enable precise momentum determination. The TPC is designed to achieve a momentum resolution of less than 125 MeV which will allow for the separation of the three Upsilon S-states [1]. The last tracking system is the TPC Outer Tracker (TPOT) which gives a final measurement point and is used to correct for space charge distortions in the TPC.

The sPHENIX electromagnetic calorimeter (EMCal) consists of wavelength shifting fibers embedded in a tungsten powder/epoxy mixture to give an energy resolution of $\sigma/E \leq 16\%/\sqrt{E} \oplus 5\%$ [4]. The hadronic calorimeters (HCal) are of a shashlik design and are positioned just inside and outside of the solenoid magnet. The inner HCal uses scintillators and aluminum plates and the outer HCal uses steel instead of aluminum. The outer HCal also doubles as the magnets flux return and the combined HCal system is designed to have $\sigma/E \leq 100\%/\sqrt{E}$.

When the approval to operate sPHENIX was given on May 18th 2023, the collaboration proceeded with commissioning the detector efficiently and methodically in stages beginning with the minimum-bias detectors and the calorimetry system. The RHIC run in 2023 was planned to continue until September 30th, but unfortunately terminated early on August 1, 2023, due to the failure of a RHIC cryogenic valve box. By this stage the calorimeters, end-cap detectors, INTT and TPOT had been commissioned and studies on the MVTX and TPC were ongoing. In spite of this early end, all subsystems had successfully recorded data and observed correlations of activity both internal to each system, and with other sPHENIX subsystems, successfully demonstrating proper operations of the DAQ system. The sPHENIX collaboration continued commissioning using cosmic rays and demonstrated correlations among the entire tracking system to be used for detector alignment.

2 Open heavy flavor at sPHENIX

The lower collision energy at RHIC compared to the LHC results in a lower mean p_T of mother particles at RHIC, and hence the majority of heavy flavor candidates collected at sPHENIX will probe the low p_T region. In this region, hadronization mechanisms such as coalescence are expected to dominate over fragmentation [5–7]. This is especially true for b -hadrons, with b -quarks having a larger mass than c -quarks and so experiencing less recoil from the medium for comparable momenta. The combination of low mean p_T , excellent DCA resolution expected from the MVTX, and the SRO system will enable precision measurements of b -hadrons in heavy ion collisions [8].

By using non-prompt D^0 decays from b -mesons, sPHENIX can measure R_{AA} and v_2 and compare them to prompt D^0 decays to provide insights into parton energy loss. If a Brownian motion-like approach is used to understand the transport of quarks through the QGP, then we can also use v_2 measurements to constrain the heavy quark diffusion coefficients. Projections for the statistical uncertainty on both of these measurements can be seen in Figure 1.

The large prompt D^0 data-set can be used to understand directed flow in both the D^0 and \bar{D}^0 systems where it is expected that the transient magnetic field will cause a splitting in the flow values as the magnetic field operator is odd under charge conjugation [10]. This measurement has been attempted before at RHIC but was statistically limited [11]. Also complicating the measurement is the need to separate the D^0 states. In the $K^\mp\pi^\pm$ final state, which has both a large branching fraction ($\sim 4\%$ [12]) and can be fully reconstructed, the D^0 undergoes mixing [13] and can decay to both final states (known as "right-sign" and "wrong-sign" decays). Techniques are being developed at sPHENIX to correct for these challenges which, if uncorrected, can dilute the splitting effect, and mask it entirely if it is small enough.

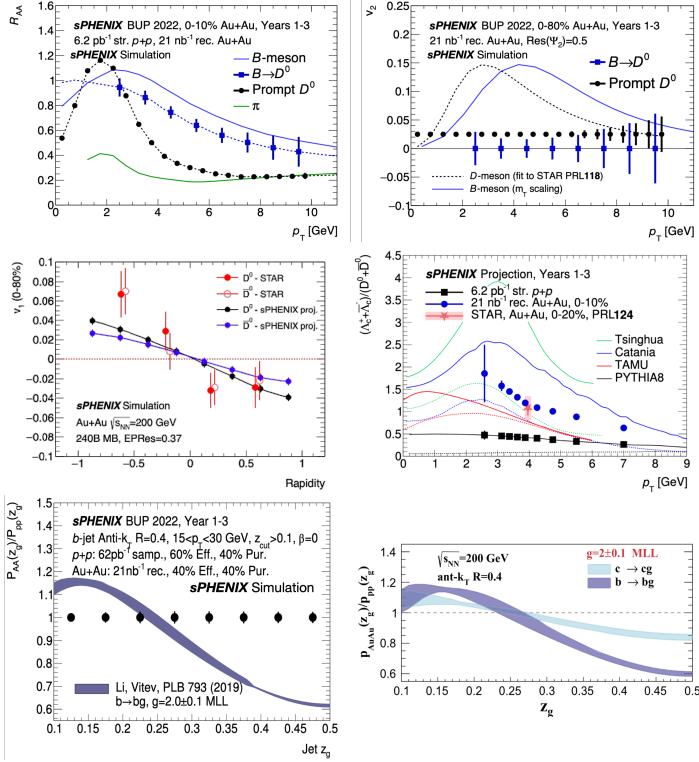


Figure 1. Projected statistical sensitivities to R_{AA} (top left) and v_2 (top right) for prompt (black) and non-prompt (blue) D^0 , sensitivities to v_1 for D^0 and \bar{D}^0 decays (middle left), sensitivity to the baryon/meson ratio in open charm decays (middle right) for $p+p$ (black) and Au+Au (blue), and sensitivity to the sub-jet splitting ratio for b -jets (bottom right) at sPHEX using 10% SRO. A comparison of the expected enhancement of the sub-jet splitting ratio for c - and b -jets can be seen in the bottom right figure where the enhancement is more prominent for b -jets [9].

The D^0 measurements can also be combined with those of Λ_c^+ to study the baryon-to-meson ratio in both $p+p$ and Au+Au. Previous studies of this ratio using light flavor decays have demonstrated an enhancement in heavy ion collisions compared to $p+p$ collisions. While the STAR collaboration observed a similar ratio in Au+Au collisions using open charm decays, there is no measurement from RHIC using a $p+p$ data set [14]. Measurements of this ratio have been performed at the LHC using Pb+Pb collisions [15–17], and SRO will allow for a measurement of this ratio in $p+p$ collisions for a direct comparison to the Au+Au and LHC results.

sPHEX also has an extensive heavy flavor jets program such as studying elliptic flow in the medium- p_T regime in the most central events. In the range from approximately 15 to 40 GeV, it is expected that the light and heavy flavor jets exhibit similar flow behavior and sPHEX will provide valuable insight as to why these behaviors converge. Another jet measurement of interest is to compare the sub-jet splitting, z_g , of b -jets in Au+Au and $p+p$ collisions. The splitting can be used as another constraint on the QGP and is expected to be more prominent for the beauty sector than for the charm sector [9].

3 AI-assisted event selection

The expectations shown in Figure 1 were produced using the expected statistics recorded with 10% SRO which is achieved by extending the readout of the tracking system up to $7\ \mu\text{s}$ after a trigger decision is received during $p+p$ collisions. The back-end electronics of the calorimeter system have a maximum trigger rate of 15 kHz which corresponds to the mean Au+Au collision rate at RHIC, whereas the $p+p$ collision rate is 3 MHz. The data volume is also dominated by the information from the TPC. Thus, it was chosen to stream for $7\ \mu\text{s}$ to avoid overfilling the data buffers. With this in mind, the fastML group is developing a system to be deployed at sPHENIX to sample the remaining 90% of $p+p$ collisions using the MVTX and INTT, perform a fast ($\sim 5\ \mu\text{s}$) tracklet reconstruction and event selection to identify potential heavy flavor decays. This demonstrator will then send a signal to the TPC to read out its data which will be saved alongside the MVTX and INTT to enhance heavy flavor statistics.

The trigger algorithms will be performed by a FELIX card housed inside a standalone server. Data will be passed optically from the MVTX and INTT back-end electronics where all the unpacking, clustering, reconstruction and decision making will be performed on the powerful FPGA in the FELIX card. Tracklet reconstruction and event determination will be achieved using graph neural networks, and thus the algorithms must be translated to a high level synthesis language. This is achieved by the hls4ml package [18] which performs this translation and synthesizes an IP block which can be placed inside a firmware design. This is advantageous as it allows algorithms to be integrated within other firmware development such as data unpacking and clustering. Another feature of hls4ml is the ability to tune an algorithm between execution speed and precision by altering the number of bits (flip-flops or FF) used in each stage of the algorithm.

Conceptually, a graph consists of a set of nodes and related nodes are connected by edges to aggregators. In our model, each node represents a track, where a track is represented by 3 MVTX and 2 INTT hits, the distance separating hits in adjacent layers, their angle and the summed length of the hit separation. The aggregators represent the vertices and the edges are used to define which tracks belong to primary or secondary vertices. The neural network passes information from the nodes to the aggregators and back, to build weights for each edge until the model builds a complete representation of the event. The event selection algorithm is still under development using a preliminary model based on secondary vertex determination. The combined tracklet reconstruction and event selection has an average processing time of $8.8\ \mu\text{s}$ with a 285 MHz clock and uses 15% of the FPGA lookup tables, 8% of FFs and 20% of block RAM. Overall this has resulted in a 91% tracklet-building efficiency for a 97% area-under-the-curve (ROC). The device aims to be deployed at sPHENIX during Run 24.

References

- [1] The sPHENIX Collaboration, *sPHENIX Technical Design Report* (2019), <https://indico.bnl.gov/event/7081/>
- [2] T. Xuan et al., Proceedings of the AAAI Conference on AI **37**, 15752 (2023)
- [3] The sPHENIX Collaboration, *MVTX Technical Design Report* (2018), <https://indico.bnl.gov/event/4072/>
- [4] C.A. Aidala et al., IEEE Transactions on Nuclear Science **68**, 173 (2021)
- [5] K. Das, R.C. Hwa, Physics Letters B **68**, 459 (1977)
- [6] R. Rapp, E.V. Shuryak, Phys. Rev. D **67**, 074036 (2003)
- [7] R.J. Fries, B. Müller, C. Nonaka, S.A. Bass, Phys. Rev. C **68**, 044902 (2003)

- [8] R. Belmont et al., arXiv **2305.15491** (2023)
- [9] H.T. Li, I. Vitev, Physics Letters B **793**, 259 (2019)
- [10] U. Gürsoy, D. Kharzeev, K. Rajagopal, Phys. Rev. C **89**, 054905 (2014)
- [11] J. Adam et al. (STAR Collaboration), Phys. Rev. Lett. **123**, 162301 (2019)
- [12] R.L. Workman et al. (Particle Data Group), PTEP **2022**, 083C01 (2022)
- [13] R. Aaij et al. (LHCb Collaboration), Phys. Rev. Lett. **127**, 111801 (2021)
- [14] J. Adam et al. (STAR Collaboration), Phys. Rev. Lett. **124**, 172301 (2020)
- [15] S. Acharya et al. (ALICE Collaboration), Physics Letters B **793**, 212 (2019)
- [16] A. Sirunyan et al. (CMS Collaboration), Physics Letters B **803**, 135328 (2020)
- [17] R. Aaij et al. (LHCb Collaboration), JHEP **06**, 132 (2023)
- [18] F. Fahim et al., arXiv **2103.05579** (2021)